THE ASTROPHYSICAL JOURNAL, 276:114–126, 1984 January 1

TWO-FLUID GRAVITATIONAL INSTABILITIES IN A GALACTIC DISK[1]

CHANDA J. JOG[2] AND P. M. SOLOMON[3]
State University of New York at Stony Brook, N. Y.
Received 1983 February 22; accepted 1983 June 13

ABSTRACT

We formulate and solve the hydrodynamic equations describing an azimuthally symmetric galactic disk as a two-fluid system. The stars and the gas are treated as two different isothermal fluids of different velocity dispersions ($C_s \gg C_g$), which interact gravitationally with each other. The disk is supported by rotation and random motion. The formulation of the equations closely follows the one-fluid treatment by Toomre. We solve the linearized perturbation equations by the method of modes, and study the stability of the galactic disk against the growth of axisymmetric two-fluid gravitational instabilities.

We find that even when both the fluids in a two-fluid system are separately stable, the joint two-fluid system, because of the gravitational interaction between the two fluids, may be unstable. The ratio of the gas contribution to the stellar contribution toward the formation of two-fluid instabilities is substantially greater than μ_g/μ_s, the ratio of their respective surface densities; this is due to the lower gas velocity dispersion as compared to the stellar velocity dispersion ($C_g \ll C_s$). The two contributions are comparable when the gas fraction (μ_g/μ_s) is only $\sim$0.10–0.25. Therefore, a galactic disk is a meaningful two-fluid system even when the gas constitutes only 10%–20% of the total surface density. The ratio of the amplitude in the gas to the amplitude in the stars is an increasing function of the wavenumber of the two-fluid perturbation.

The wavelength and the time of growth of a typical two-fluid instability in the inner galaxy, for $\mu_g/\mu_s = 0.1$–0.2, and $\sim$2–3 kpc and ~ 2–4×10^7 years, respectively, and each of these contains gas of mass 4×10^7–$10^8\ M_\odot$.

The two-fluid analysis presented here is applicable to any general disk galaxy consisting of stars and gas.

Subject headings: galaxies: internal motions — galaxies: structure — instabilities — interstellar: matter

I. INTRODUCTION

a) *Observations and Motivation for the Two-Fluid Analysis*

In the past seven years there has been a substantial revision in the determination of the spatial distribution, mean density, and mass of interstellar matter in the Galaxy. This is primarily due to millimeter wave observations of CO emission throughout the galactic plane which have shown that molecular clouds (clouds in which the hydrogen is primarily H_2) contain a substantial portion of the total interstellar matter (Scoville and Solomon 1975; Gordon and Burton 1976); these clouds are concentrated in the inner Galaxy with a peak at a galactocentric radius, R, of 6 kpc (declining by a factor of 4 out to the solar radius of 10 kpc, completely unlike atomic hydrogen which varies only slightly from $R = 5$ to $R = 10$ kpc). The molecular cloud distribution also has an inner edge between 3 and 4 kpc with a minimum between 1.5 and 3 kpc. (We exclude the galactic center from discussion here.)

The average gas density in the inner Galaxy is much higher than previously believed based on H I data alone which showed only $\sim$0.4–0.5 H atoms cm^{-3}. The average H_2 density based on ^{13}CO observations has been estimated at the peak of the distribution to be 2.5 cm^{-3} by Solomon, Scoville, and Sanders (1979) and by Liszt and Burton (1981). A recent determination of the density and scale height of the H_2 distribution (Sanders, Solomon, and Scoville 1984) shows that the surface density of molecular clouds is about 22 $M_\odot$ pc^{-2} at the peak of the distribution, or between 10% and 15% of the total surface density estimated from dynamical models; this is to be compared with 5 $M_\odot$ pc^{-2} or 2–3% that was previously found from H I alone. The scale height of the H_2 is about half that of H I. The recent CO observations of external galaxies such as NGC 6936, IC342, M101, and NGC 891 (Young and Scoville 1981, 1982; Solomon 1981; Solomon *et al.* 1983) show that the inner 5–7 kpc region has a very high surface density of H_2, with H_2 exceeding H I by as much as an order of magnitude. Thus the quantity and the form of interstellar matter in many galaxies are substantially different from those expected based on H I data alone.

The chief characteristic of interstellar molecular matter, in addition to its galactic distribution, is the confinement of most of the mass to giant molecular clouds with individual masses in the range 10^5–$3 \times 10^6\ M_\odot$, sizes between 20 and 80 pc, and H_2 density of 300 cm^{-3} (Solomon, Sanders, and Scoville 1979; Solomon and Sanders 1980). Stark (1979), and Liszt and Burton (1981) find a similar distribution of cloud masses with slight differences at the low end. However, the main characteristic—namely, that most of the mass is in the very massive clouds—is agreed upon by all observers. These objects are themselves held together by gravity rather than by pressure equilibrium with an external intercloud medium. There is in addition a tendency of even these giant clouds to cluster in regions of several hundred parsecs (Sanders and Solomon 1984), although a full analysis is not available.

[1] This paper is based on a dissertation submitted by one of the authors (C. J. Jog) to the State University of New York at Stony Brook in partial fulfillment of the requirements for the Ph.D. degree.

[2] Department of Physics, SUNY Stony Brook.
[3] Astronomy Program, SUNY Stony Brook and Institute of Astronomy, Cambridge, England.

In the past, *nongravitational* agglomeration models for the buildup of gas clouds have been studied by Kwan (1979), Scoville and Hersh (1979), and Cowie (1980). Cowie's model depends crucially on the existence of an underlying large-scale spiral potential in the disk. These authors were interested in the buildup of individual gas clouds ($M_{\rm cloud} \sim 10^5\ M_\odot$ and $\lambda \lesssim 50$–60 pc). Elmegreen has developed gravitational models that also employ a large-scale spiral potential (Elmegreen 1979) and magnetic fields (Elmegreen 1982*a*, *b*) for obtaining cloud clusters. Technically, both these models have restricted spatial applicability in the disk.

The large average gas densities and segregation into massive, dense objects suggest that self-gravitational forces in the interstellar gas itself may be responsible for the formation of these clouds and consequent star formation. Yet when one applies the necessary criterion for the growth of gravitational instabilities in a fluid (Goldreich and Lynden-Bell 1965; Toomre 1964), one finds that the gas, at the average spread-out density and observed velocity dispersion, would be stable (see Appendix A for the details). The average gas density, however, needs to be increased by only a small factor (~ 2)—the actual value depends on the gas velocity dispersion—before the gas becomes susceptible to the formation of instabilities in it.

Now, the stars constitute the largest mass component of the galactic disk, and therefore it is compelling to study the effect on gas of the (stellar) gravitational potential associated with the azimuthally symmetric distribution of stars in the disk. Conversely, the existence of a significant mass fraction in a cold fluid (the molecular ISM or the total ISM) will influence the stability of the entire galactic disk including the stars. The gravitational interaction of these two fluids may play a determining role in the structure and evolution of galactic disks. This is the primary motivation for this study.

In this paper we formulate the two-fluid scheme and obtain the characteristics of two-fluid gravitational instabilities in a galactic disk. In a subsequent paper (Jog and Solomon 1984, Paper II), we investigate the critical stellar velocity dispersions and the formation of condensations in the gas in a two-fluid galactic disk.

b) Contents

We approximate a galactic disk as a two-fluid system wherein the stars are represented as an isothermal fluid and the interstellar gas is represented as another isothermal fluid; the two fluids interact gravitationally with each other. The disk is supported by rotation and random motion.

In § II, we formulate the hydrodynamic equations describing the above two-fluid system for the local, axisymmetric ($m = 0$) case. We solve the linearized perturbation equations by the method of modes and obtain the dispersion relation for the two-fluid system. We thus obtain the instability criterion for two-fluid gravitational instabilities. The main result from these calculations is that even when neither fluid is unstable by itself, the two-fluid system—because of the additional gravitational self-energy in the system resulting from the gravitational interaction between the two fluids—may be unstable.

In § III we study the characteristics of the two-fluid gravitational instabilities, and obtain the growth rate and the wavelength for the fastest growing perturbation at a particular region in the Galaxy. We show that both the growth rate and $\Delta\lambda$, the range of unstable wavelengths, are sharply increasing functions of the fractional gas content in the disk. We also compare a galactic disk treated first as a two-fluid system with a disk consisting of two separate one-fluid systems. Next, we study the relative contribution of the two fluids toward the formation of the two-fluid gravitational instabilities. We find that the ratio of the gas contribution to the stellar contribution is much higher than the ratio of their surface densities. Finally, we study the ratio of the amplitudes in the two fluids as a function of the wavenumber of the two-fluid perturbation.

Section IV contains a summary of the conclusions from this paper.

Although the main motivation for this work was provided by the observation of a widespread, clumpy gas distribution (giant molecular clouds) in the Galaxy, the analysis presented here deals with the entire two-fluid disk, and we treat both the stars and the gas on an equal basis.

II. DERIVATION OF THE INSTABILITY CRITERION FOR TWO-FLUID GRAVITATIONAL INSTABILITIES IN A GALACTIC DISK

In this section we formulate the equations describing a system consisting of two fluids which interact gravitationally with each other. Next, we solve these equations in order to study the gravitational stability of such a system.

a) Physical Parameters of the Disk

We assume that the stars in the galactic disk form an isothermal fluid characterized by the following three parameters: μ_s, the stellar surface density; C_s, the isothermal sound speed in the stellar fluid; and $2h_s$, the z-scale height of the stellar mass distribution. Similarly, the gas is assumed to be another isothermal fluid characterized by the corresponding parameters μ_g, C_g, and $2h_g$.

We assume that hydrodynamic equations describe the collective stellar dynamic behavior. The use of the hydrodynamic equations, and in particular the use of an isotropic planar pressure term to describe the random motion of particles in a collisionless system, is justified by the excellent qualitative agreement and the substantial quantitative agreement between a hydrodynamic approach and a distribution function approach for treating the collective particle dynamical behavior (Berman and Mark 1977 and references therein). The main motivation for using the hydrodynamic approach for the stellar fluid is the inherent simplicity involved since one then has to deal only with the first two moments of the Boltzmann equation.

We assume that the two fluids are distributed geometrically in an infinitesimally thin disk which features both differential rotation and random motion. The two fluids corotate with each other. We do the local, linear axisymmetric perturbation analysis for such a system.

We use the nonrotating cylindrical polar coordinates, r, θ, z such that the $z = 0$ plane coincides with the central plane of the disk, $r = 0$ coincides with the rotation axis, and θ is taken to be increasing along the direction of rotation. The unperturbed angular velocity, surface density, and gravitational potential are denoted by $\Omega_0(r)$, $\mu_0(r)$, and $\phi_0(r)$, respectively. We consider the perturbations which involve

no motion in the z-direction. The perturbed quantities will be denoted by $\delta\mu(r, \theta, t)$, $\delta\phi(r, \theta, t)$, $u(r, \theta, t)$, and $v(r, \theta, t)$, where u and v respectively denote the radial and the circumferential disturbance velocity components. The above perturbed quantities, with the exception of $\delta\phi$, when accompanied by the subscripts g and s, respectively represent the parameters describing the gas and the stellar fluid. The unperturbed surface densities for the gas and the stellar fluid are given as μ_{g0} and μ_{s0} respectively.

The constituents of both the fluids undergo the elliptic-epicyclic orbits under the general galactic rotation law. The epicyclic frequency, κ, is defined as:

$$\kappa^2 = 4B(B - A)\,, \tag{1}$$

where A and B are the Oort constants, derived locally at each r, and are defined as:

$$A(r) = \tfrac{1}{2}[\Omega_0(r) - dV(r)/dr]\,,$$
$$B(r) = \tfrac{1}{2}[\Omega_0(r) + dV(r)/dr]\,, \tag{2}$$

where $V(r)$ is the linear velocity of revolution and equals $r[\Omega_0(r)]$.

The following seven equations (3)–(9)—where $i = s$ and g yield equations (3), (5), (7) and (4), (6), (8), respectively—are the linearized hydrodynamic equations for the two-fluid gravitationally interacting system and govern the small perturbation to the same:

$$\partial_t u_i + \Omega_0(r)\partial_\theta u_i - 2\Omega_0(r)v_i + (C_i^2\partial_r \delta\mu_i)/\mu_{i0}(r) + [\partial_r(\delta\phi_s + \delta\phi_g)]_{z=0} = 0\,, \quad (3), (4)$$

$$\partial_t v_i - 2B(r)u_i + \Omega_0(r)\partial_\theta v_i + \{[\partial_\theta(\delta\phi_s + \delta\phi_g)]_{z=0}\}/r = 0\,, \quad (5), (6)$$

$$\partial_t \delta\mu_i + \Omega_0(r)\partial_\theta \delta\mu_i + \partial_r[\mu_{i0}(r)u_i] + [\mu_{i0}(r)u_i]/r + [\mu_{i0}(r)\partial_\theta v_i]/r = 0\,, \quad (7), (8)$$

$$\{[\partial_r r\partial_r(\delta\phi_s + \delta\phi_g)]/r\} + \partial_z{}^2(\delta\phi_s + \delta\phi_g) = 4\pi G(\delta\mu_s + \delta\mu_g)\delta(z)\,. \tag{9}$$

Here, $\delta(z)$ is the Dirac delta-function; the gravitational force per unit mass is given by the positive gradient of ϕ.

Equations (3) and (5) are the radial and the azimuthal force equations, respectively, for the stellar fluid; and equations (4) and (6) are the same for the gas. Note that each fluid experiences the joint gravitational perturbation potential $(\delta\phi_s + \delta\phi_g)$ due to both the fluids.

The continuity equations for the stellar fluid and the gas are given respectively by equations (7) and (8); these are taken to be independent since we expect little interconversion of the material in the two fluids on a dynamical time scale. Equation (9) is the joint Poisson equation for this gravitationally interacting two-fluid system.

b) *Solution of the Local, Linearized Perturbation Equations: Derivation of the Dispersion Relation*

Equations (3)–(9) are linear and homogeneous; therefore, linear superpositions of solutions is allowed and these equations can be solved by the method of modes.

We consider the axisymmetric ($m = 0$) case, hence the terms involving derivatives with respect to θ, in equations (3)–(9), are set equal to zero. The trial solution for the perturbed surface densities and the velocity dispersions is taken to be their respective magnitudes, u_g', v_g', $\delta\mu_g'$, u_s', v_s', $\delta\mu_s'$—which are small complex constants—multiplied by $\{\exp[i(kr + \omega t)]\}$, where ω is the angular frequency and k $(=2\pi/\lambda)$ is the wavenumber, which is so chosen that $kr_0 \gg 2\pi$, in accordance with the local nature of the perturbation scheme. This choice of identical wavenumber k and identical angular frequency ω, in the trial solution for the perturbed parameters of each fluid, enables us to consider the perturbations to the joint two-fluid system.

With the above choice of trial solution, the Poisson equation (eq. [9]) reduces (see Toomre 1964) to the following form:

$$[\partial_r(\delta\phi_s + \delta\phi_g)]_{z=0} = [-i2\pi G(\delta\mu_s + \delta\mu_g)]\,. \tag{10}$$

With the above choice of trial solution and the form of Poisson equation given by equation (10), equations (3)–(8) reduce to:

$$i\omega u_i' - 2\Omega_0(r)v_i' - i2\pi G(\delta\mu_s' + \delta\mu_g') + (ikC_i{}^2\delta\mu_i')/\mu_{i0} = 0\,, \quad (11), (12)$$

$$i\omega v_i' - 2Bu_i' = 0\,, \quad (13), (14)$$

$$i\omega\delta\mu_i' + ik\mu_{i0}u_i' = 0\,, \quad (15), (16)$$

where $i = s$ and g give equations (11), (13), (15) and (12), (14), (16), respectively. Solving equations (11)–(16) simultaneously, we obtain the dispersion relation for the two-fluid system, which is given next:

$$(\omega^2 - \kappa^2 - k^2C_s{}^2 + 2\pi Gk\mu_{s0})(\omega^2 - \kappa^2 - k^2C_g{}^2 + 2\pi Gk\mu_{g0}) - (2\pi Gk\mu_{s0})(2\pi Gk\mu_{g0}) = 0\,. \tag{17}$$

The first set of parentheses in the first term in equation (17) is clearly recognized as the dispersion relation for the stellar fluid by itself (see Toomre 1964 for the dispersion relation obtained for $C_s = 0$ case). Similarly, the second set of parentheses contains the dispersion relation for the gas alone (Lynden-Bell 1967; Hunter 1972; these authors assume uniform rotation, hence they get $4\Omega^2$ instead of κ^2 in the dispersion relation).

c) *The Two-Fluid Instability Criterion*

When $\omega^2 > 0$, the perturbations are oscillatory; conversely, when $\omega^2 < 0$, the perturbations are unstable, in that they have an unlimited growth. We next solve equation (17) to obtain ω^2 and thus find the unstable modes for the two-fluid system. Let

$$\kappa^2 + k^2C_s{}^2 - 2\pi Gk\mu_{s0} = \alpha_s\,,$$
$$\kappa^2 + k^2C_g{}^2 - 2\pi Gk\mu_{g0} = \alpha_g\,,$$
$$2\pi Gk\mu_{s0} = \beta_s\,,$$
$$2\pi Gk\mu_{g0} = \beta_g\,. \tag{18}$$

With the above definitions, α_s and α_g are the solutions for ω^2 in the star-alone and gas-alone cases. Thus $\alpha_s < 0$ implies that instabilities can exist in the stellar fluid by itself; similarly, $\alpha_g < 0$ implies that instabilities can exist in the gas by itself.

On substituting equation (18) into equation (17), the two-fluid dispersion relation reduces to:

$$(\omega^2 - \alpha_s)(\omega^2 - \alpha_g) - \beta_s \beta_g = 0 ,$$

that is,

$$\omega^4 - \omega^2(\alpha_s + \alpha_g) + (\alpha_s \alpha_g - \beta_s \beta_g) = 0 .$$

This is a quadratic equation in ω^2, and on solving it we get:

$$\omega^2 = \omega^2(k) = \tfrac{1}{2}\{(\alpha_s + \alpha_g) \pm [(\alpha_s + \alpha_g)^2 - 4(\alpha_s \alpha_g - \beta_s \beta_g)]^{1/2}\} . \quad (19)$$

The additive root for $\omega^2(k)$ always leads to a positive quantity, hence it indicates oscillatory perturbations under all conditions; this can be clearly seen if we check the extreme case when both fluids are unstable separately. In this case, $\alpha_s < 0$ and $\alpha_g < 0$, which (on substituting for α_s, α_g, β_s, β_g from eq. [18]) means that

$$\alpha_s \alpha_g - \beta_s \beta_g = [(\kappa^2 + k^2 C_s^2)\alpha_g - (\kappa^2 + k^2 C_g^2)\beta_s] < 0 .$$

Equation (19) then gives a positive value for the additive root of ω^2. In order to study the stability of the two-fluid system, we therefore only consider the other solution for $\omega^2(k)$, which is:

$$\omega^2(k) = \tfrac{1}{2}\{(\alpha_s + \alpha_g) - [(\alpha_s + \alpha_g)^2 - 4(\alpha_s \alpha_g - \beta_s \beta_g)]^{1/2}\} . \quad (20)$$

This solution clearly shows a most interesting result for the instability criterion. The perturbation to the joint two-fluid system will be unstable, that is, $\omega^2(k) < 0$, when

$$(\alpha_s \alpha_g - \beta_s \beta_g) < 0 . \quad (21)$$

From equation (21) it is clear that even when neither fluid is unstable by itself to the growth of the perturbation (k, ω) so that $\alpha_s > 0$ and $\alpha_g > 0$, the joint two-fluid system could still be unstable to the same perturbation. Clearly, the gravitational interaction between the two fluids is responsible for this additional help in establishing the two-fluid instabilities. When either of the two fluids is in neutral equilibrium, so that $\alpha_s = 0$ or $\alpha_g = 0$, the two-fluid system is unstable. This can be easily verified by substituting, say, $\alpha_s = 0$ in equation (20). Also, note that equation (21) gives the correct single-fluid instability criterion in the limit of very low surface density for the second fluid. For example, consider the case of very low gas density, that is, $\mu_g \to 0$, giving $\beta_g \to 0$. On substituting this value of β_g into equation (21), the instability criterion becomes $\alpha_s \alpha_g < 0$. From the definitions in equation (18), $\alpha_g = \kappa^2 + k^2 C_g^2 > 0$. Therefore equation (21) reduces to $\alpha_s < 0$, which is the one-fluid instability criterion for a stellar disk. On doing further algebraic manipulations, the two-fluid condition represented by equation (21) reduces to a physically more transparent form:

$$\frac{2\pi G k \mu_{s0}}{\kappa^2 + k^2 C_s^2} + \frac{2\pi G k \mu_{g0}}{\kappa^2 + k^2 C_g^2} > 1 . \quad (22)$$

The relative contribution of each fluid to the instability is clearly seen to be proportional to the surface density weighted with the inverse of the effective velocity dispersion. Thus a substantial contribution to the instability may be achieved by a gaseous component with a low velocity dispersion or even by a low velocity dispersion stellar component. *The form of equation (22) clearly demonstrates that the combined two fluids in a two-fluid system may be unstable even when both fluids are separately stable.*

d) *The Effects of a Finite Disk Height*

The perturbation analysis in § II*b* needs modification when account is taken of the height of the disk, which, although finite, is still much smaller than the wavelength of the perturbation.

The rotation and the random motion limited to the plane of the disk are not affected by the finite height of the disk, since the z-motion is unrelated to the motion in the plane of the disk. The finite disk height, however, does result in a reduction of the gravitational potential at $z = 0$, which is equivalent to an effective reduction in μ (Toomre 1964) by a factor $\{[1 - \exp(-kh)]/kh\}$, where $2h$ and k are respectively the total scale height of the fluid and the wavenumber of the perturbation.

It is a simple matter to see that even for the two-fluid case, finite scale heights $2h_s$ and $2h_g$ for the stellar fluid and the gas, respectively, lead to an effective decrease in the surface density of the respective fluid by a factor $\{[1 - \exp(-kh_s)]/kh_s\}$ and $\{[1 - \exp(-kh_g)]/kh_g\}$, respectively.

The modified form of equation (20) that takes account of the reduction in the effective surface densities of the fluids due to their finite scale heights is

$$\omega^2(k) = \tfrac{1}{2}\{(\alpha_s' + \alpha_g') - [(\alpha_s' + \alpha_g')^2 - 4(\alpha_s'\alpha_g' - \beta_s'\beta_g')]^{1/2}\} , \quad (23)$$

where

$$\begin{aligned} \alpha_s' &= \kappa^2 + k^2 C_s^2 - 2\pi G k \mu_{s0}\{[1 - \exp(-kh_s)]/kh_s\} , \\ \alpha_g' &= \kappa^2 + k^2 C_g^2 - 2\pi G k \mu_{g0}\{[1 - \exp(-kh_g)]/kh_g\} , \\ \beta_s' &= 2\pi G k \mu_{s0}\{[1 - \exp(-kh_s)]/kh_s\} , \\ \beta_g' &= 2\pi G k \mu_{g0}\{[1 - \exp(-kh_g)]/kh_g\} . \end{aligned} \quad (24)$$

When $\mu_{g0} = 0$,

$$\omega^2(k) = \alpha_s' , \quad (25)$$

which is the one-fluid dispersion relation for the stellar system (finite height case). Similarly, when $\mu_{s0} = 0$,

$$\omega^2(k) = \alpha_g' . \quad (26)$$

which is the one-fluid dispersion relation for the gas (finite height case).

With the finite height correction, equation (22) becomes

$$\frac{2\pi G k \mu_{g0}}{\kappa^2 + k^2 C_g^2}\left|\frac{[1 - \exp(-kh_g)]}{kh_g}\right| + \frac{2\pi G k \mu_{s0}}{\kappa^2 + k^2 C_s^2}\left|\frac{[1 - \exp(-kh_s)]}{kh_s}\right| > 1 . \quad (27)$$

The effect of the different scale heights on the validity of the two-fluid perturbation analysis is discussed in Appendix B.

III. CHARACTERISTICS OF THE TWO-FLUID GRAVITATIONAL INSTABILITIES

We first describe the values assigned to the various input parameters (§ III*a*). In § III*b*, we plot the function $\omega^2(k)$ (as

given in eq. [23], § II*d*) versus k [or, equivalently, $\omega^2(k)$ vs. λ^{-1}] to investigate its general behavior and to study the characteristics of the resulting two-fluid instabilities. We also compare the differences between a galactic disk treated first as a two-fluid system and then as consisting of two separate (noninteracting) one-fluid systems. In § III*c* we discuss the relative contribution from the two fluids as a function of μ_g/μ_s and k. In § III*d*, we plot ω^2 versus λ^{-1} for a two-fluid case which has four real k roots. In § III*e* we study the ratio of the amplitudes in the two fluids as a function of k.

While we adopt the rotation curve for the Galaxy, we vary the values assigned to some parameters (in particular the ratio of the gas surface density to the stellar surface density) beyond their observed values. Hence the general results derived in this section are applicable to any disk galaxy.

a) Description of the Parameters in the Galaxy

The input parameters are: the epicyclic frequency κ, and the surface densities and velocity dispersions and scale heights for the stars and the gas—that is, μ_s, C_s, $2h_s$, μ_g, C_g, $2h_g$.

The values of κ, the epicyclic frequency, and μ_t $(=\mu_s + \mu_g)$, the total disk surface density, as functions of R, the galactocentric radius, are adapted from the model of Caldwell and Ostriker (1981). The actual value of $\mu_t(R)$ may be uncertain at $R \sim 5$ kpc by as much as 40–50% as shown by the difference between the above model and those of Innanen (1973).

Between $R \sim 5$ and 10 kpc, the observed average gas surface densities in the galaxy (Sanders 1982; Sanders, Solomon, and Scoville 1984), including both H_2 and H I corrected for helium, fall in the range of 12–15% of the adopted total disk surface density. This includes about two hydrogen molecules per cm^3 as the average density at the midplane between $R = 5$ and 8 kpc, a HWHM in z of 60 pc, yielding $\langle\mu_g(H_2)\rangle = 14\ M_\odot\ \mathrm{pc}^{-2}$ and $3.5\ M_\odot\ \mathrm{pc}^{-2}$ for H I. At $R = 6 \pm 0.5$ kpc, $\mu_g(H_2) = 22\ M_\odot\ \mathrm{pc}^{-2}$. These densities are uncertain by about 50%, primarily because of uncertain conversion factors for translating ^{12}CO and ^{13}CO observations to molecular hydrogen densities. However, the range of conversion factors measured by various techniques restricts the mean H_2 surface density to within a factor of 2 of the value quoted above (Sanders, Solomon, and Scoville 1984; Liszt and Burton 1981). For the purpose of this paper, we simply consider gas surface densities ranging between 10% and 20% of the stellar surface density $(\mu_g/\mu_s = 0.1\text{–}0.2)$. Table 1 shows the actual densities used in our calculations.

We assume that the entire stellar component, with stellar surface density containing all of the nongaseous disk density, μ_s $(=\mu_t - \mu_g)$, can be characterized by a single velocity dispersion, C_s. While the actual stars in the disk have a range of velocity dispersions, we approximate the stars as one component in order to demonstrate the effect of the very low velocity dispersion gas.

The values of C_s and $2h_s$ are known observationally only for the solar neighborhood. One can, however, theoretically obtain C_s as a function of h_s or vice versa by noting that the disk has to be in pressure equilibrium. We adopt the disk pressure equilibrium criterion (DPEC) (see, e.g., Talbot and Arnett 1975). For a system consisting of n-fluids, the DPEC is given as

$$\frac{C_i}{h_i} = \pi G \sum_n \left(\frac{\mu_n}{C_n}\right). \tag{28}$$

This criterion is applicable to a system of two or more fluids whether or not the two (or more) fluids interact with each other. Equation (28) is valid for the z-component of velocity dispersion, whereas we need to use the planar stellar velocity dispersion in the perturbation calculations for the two-fluid system. In the solar neighborhood, the typical value for $(C_s)_{\mathrm{planar}}/(C_s)_z \sim 1.75$ (Mihalas and Binney 1981), where $(C_s)_{\mathrm{planar}}$ is taken to be the average of the stellar dispersion along the $\hat{r}$ and $\hat{\theta}$ directions. We adopt this conversion ratio at all R.

C_g, the sound speed in gas, is equal to the one-dimensional cloud-cloud velocity dispersion. From H I observations, C_g is typically ~ 8 km s^{-1} (Spitzer 1978); and from H_2 observations, a whole range of values from 4 km s^{-1} (Stark 1979; Liszt and Burton 1981) to 8 km s^{-1} (Stark 1979) have been suggested for C_g in the plane. From the gaseous H_2 scale height, Sanders, Solomon, and Scoville (1984) have found $C_g = 4.9$ km s^{-1}. It turns out that the actual value chosen for C_g (from the above suggested range) is immaterial for most of the two-fluid cases considered here because $k^2 C_g^{\,2} \ll \kappa^2$ for the values of k of interest. We have set $C_g = 5$ km s^{-1}.

Solomon, Sanders, and Scoville (1979) find the H_2 gas scale height (HWHM) to be approximately constant or slowly increasing with R for $4.5 < R < 8.5$ kpc with a mean value of (60 ± 9) pc. In our calculations, we set $2h_g$, the total scale height, to be equal to the total scale height corresponding to an $1/e$ falloff in the gas surface density and hence $2h_g = 2(\mathrm{HWHM})/0.83 \approx 150$ pc.

b) ω^2 vs. λ^{-1} Plots: Comparison of Two-Fluid and One-Fluid Cases

Each curve labeled S + G in Figures 1–2 represents a plot of ω^2 versus λ^{-1} for a two-fluid system, calculated

TABLE 1

ADOPTED PARAMETERS OF THE DISK

			$\mu_g/\mu_s = 0.1$		$\mu_g/\mu_s = 0.15$		$\mu_g/\mu_s = 0.2$	
R (kpc)	κ[a] (km s^{-1} kpc^{-1})	μ_t[a] $= \mu_g + \mu_s$ ($M_\odot$ pc^{-2})	μ_s ($M_\odot$ pc^{-2})	μ_g ($M_\odot$ pc^{-2})	μ_s ($M_\odot$ pc^{-2})	μ_g ($M_\odot$ pc^{-2})	μ_s ($M_\odot$ pc^{-2})	μ_g ($M_\odot$ pc^{-2})
6	65	209	190.0	19.0	181.7	27.3	174.2	34.8
10	39	82	74.5	7.5	71.3	10.7	68.3	13.7

[a] The values for κ and μ_t are from Caldwell and Ostriker 1981.

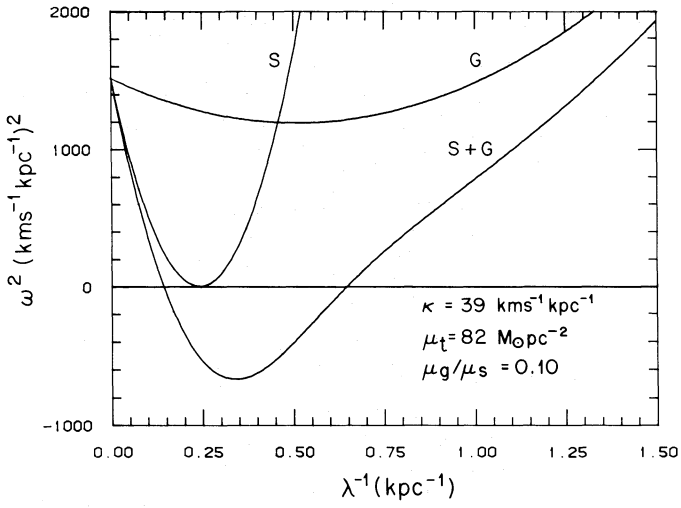

FIG. 1a

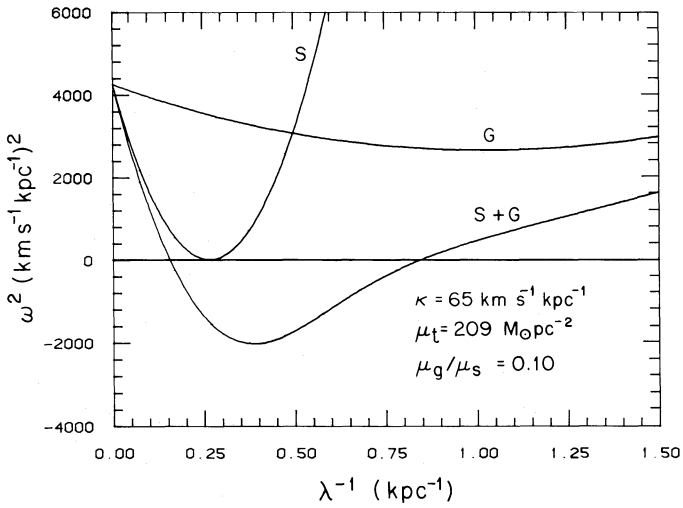

FIG. 1b

FIG. 1.—ω^2 versus λ^{-1}, for the stars-alone (S), the gas-alone (G) and the two-fluid (S + G) systems, when stars-alone system is in neutral equilibrium, $\mu_g/\mu_s = 0.1$. (*a*) $\kappa = 39$ km s^{-1}, $\mu_t = 82\ M_\odot$ pc^{-2}, $C_s = 22.8$ km s^{-1}. (*b*) $\kappa = 65$ km s^{-1} kpc^{-1}, $\mu_t = 209\ M_\odot$ pc^{-2}, $C_s = 34.7$ km s^{-1}. These parameters correspond approximately to conditions at $R \sim 10$ kpc and 6 kpc, respectively. $C_g = 5$ km s^{-1}. Even when one component fluid is neutrally stable and the other is stable, the joint two-fluid system is unstable. The growth rate of the most unstable mode, ω_{peak}, is higher at $R = 6$ kpc (Fig. 1*b*) than at $R = 10$ kpc (Fig. 1*a*).

using equation (23). Each curve labeled S or G in these figures represents the one-fluid dispersion relation for the stellar fluid alone or the gas alone (eq. [25] or [26]), respectively. For each curve, the perturbation mode (k, ω) is unstable when $\omega^2(k) < 0$ (see § IIc). The subcases *a* and *b* in Figures 1–3 refer to galactic parameters at $R \simeq 10$ kpc and 6 kpc, respectively.

Figures 1 and 2 assume $\mu_g/\mu_s = 0.1$. The curve labeled S + G representing the interacting two-fluid case is drawn at a total surface density, μ_t, equal to the sum of the surface densities used for curve S and curve G ($\mu_t = \mu_g + \mu_s$). In Figure 1, C_s is determined, for both curves S and S + G, by requiring that the stellar system by itself be in neutral equilibrium. Figure 2 is similar to Figure 1, but both curves S and S + G are determined by requiring that the two-fluid system (curve S + G) be in neutral equilibrium. Thus, Figures 1 and 2 represent the same systems, but with different stellar velocity dispersions. (C_s is determined numerically by plotting eq. [25] for Fig. 1 and eq. [23] for Fig. 2 and ensuring that the two real k roots are nearly

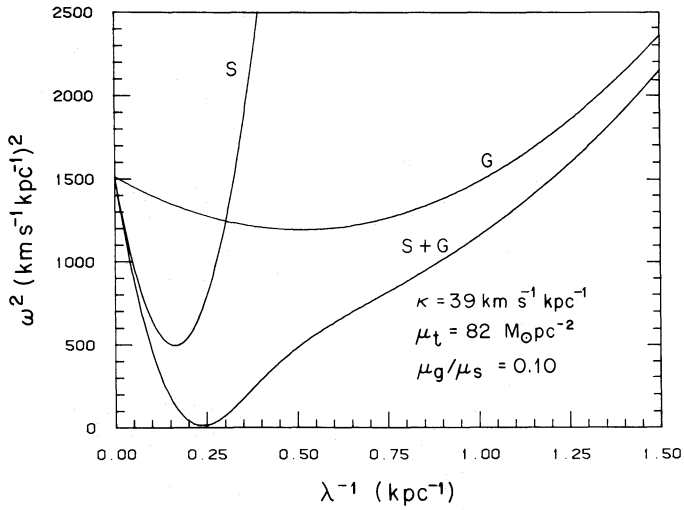

FIG. 2a

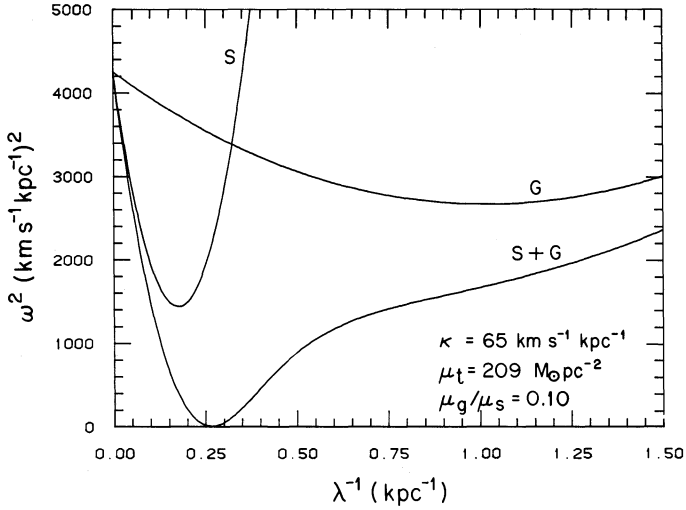

FIG. 2b

FIG. 2.—ω^2 vs. λ^{-1}, for the stars-alone (S), the gas-alone (G), and the two-fluid (S + G) systems, when the two-fluid system is in neutral equilibrium. $\mu_g/\mu_s = 0.1$. In (*a*) $\kappa = 39$ km s^{-1} kpc^{-1}, $\mu_t = 82\ M_\odot$ pc^{-2}, $C_s = 27.8$ km s^{-1}. (*b*) $\kappa = 65$ km s^{-1} kpc^{-1}, $\mu_t = 209\ M_\odot$ pc^{-2}, $C_s = 42.6$ km s^{-1}. These parameters correspond approximately to conditions at $R \sim 10$ kpc and 6 kpc, respectively. $C_g = 5$ km s^{-1}. Even when both the fluids are separately stable, the joint two-fluid system is in neutral equilibrium.

coincident. A detailed discussion of neutral equilibrium is given in Paper II [Jog and Solomon 1984].)

In each figure, the value of h_s used in drawing curves S and S + G is evaluated self-consistently using DPEC for a system of one fluid ($n = 1$, eq. [28]) and a system of two fluids ($n = 2$, eq. [28]).

For the sake of convenience, we assume constant $2h_g$ ($=0.15$ kpc) and C_g ($=5$ km s^{-1}) for all cases. This is justified because kh_g is small (~ 0.2) for the values of k of interest and hence the finite height reduction factor for gas (eq. [24], § II*d*) is ~ 1.

The effect of the gravitational interaction between the two fluids is substantial, as can be readily seen in Figures 1 and 2. From Figure 1, we see that even when the stellar fluid is neutrally stable and the gas is stable, the joint two-fluid system—because of the gravitational interaction between the two fluids—does exhibit instabilities. From Figure 2, we can see that when the two-fluid system is just neutrally stable, both the fluids would be stable when considered separately. These two results confirm the similar results (namely, that eq. [21] may be satisfied even when $\alpha_g > 0$ and/or $\alpha_s > 0$) derived analytically in § II*c* for a thin disk case. Thus, the two-fluid system is more unstable (or tends to be more unstable) than either of its component fluids.

The two-fluid instabilities in Figure 1 are limited to a certain range over k; the range is rotation-limited at the lower k end and pressure-limited at the larger k end. This behavior is also seen in the case of one-fluid instabilities (Toomre 1964; Goldreich and Lynden-Bell 1965).

The rate of growth for a given unstable mode (k, ω) is equal to $[-\omega^2(k)]^{1/2}$; call this $|\omega|$. T_e, the e-folding time, that is, the time required for growth by a factor e in the density, is given by $T_e = [(10^9/1.0227) \times 1/|\omega|]$ years, where ω is given in units of km s^{-1} kpc^{-1}. For a given set of values for the input parameters, let $\omega_{\rm peak}$ and $k_{\rm peak}$ specify the growth rate and the wavenumber, respectively, for the fastest growing mode; clearly, this is the mode of interest in the local, linear, axisymmetric perturbation analysis such as the one considered in this paper.

From Figure 1*a* we obtain $k_{\rm peak} = 2.5$ kpc^{-1} and $\omega_{\rm peak} = 24.9$ km s^{-1} kpc^{-1} so that $T_e = 3.9 \times 10^7$ yr. From Figure 1*b*, we obtain $k_{\rm peak} = 3.1$ kpc^{-1} and $\omega_{\rm peak} = 42.0$ km s^{-1} kpc^{-1} so that $T_e = 2.5 \times 10^7$ yr. Note that $\omega_{\rm peak}$, the rate of fastest growth, is greater at $R = 6$ kpc than it is at $R = 10$ kpc; this is because the growth rate depends on the absolute values of the surface densities of the gas and the stellar fluid, both of which increase at lower R values.

A better demonstration of the effect of the gas on the gravitational stability is obtained by comparing a one-fluid stellar system with a two-fluid system which has the identical total surface density. In Figure 3, the stellar density $(\mu_s)_{1\text{-}f}$ used in calculating the stellar fluid dispersion relation is equal to the total surface density $(\mu_t)_{2\text{-}f}$ used in plotting each of the two-fluid curves. The ratio μ_g/μ_s is set equal to 0.1, 0.15, and 0.2, respectively in the three two-fluid curves. The curve with $\mu_g/\mu_s = 0$ is drawn for the case when the stellar system [with $(\mu_s)_{1\text{-}f} = (\mu_t)_{2\text{-}f}$] is in neutral equilibrium. The same value of C_s is used in drawing each of the two-fluid curves. The curve with $\mu_g/\mu_s = 0$ here can be thought of as an extreme case of a two-fluid system where $\mu_g/\mu_s = 0$.

From Figure 3, we can see that even when a small fraction (~ 0.10) of the density of a neutrally stable stellar system is put in a cold fluid (that is, gas), the resulting two-fluid system is unstable to the growth of perturbations over a wide range of wavelengths.

The ratio μ_g/μ_s is a very important parameter in this scheme. The maximum growth rate of the resulting two-fluid instability is an increasing function of μ_g/μ_s, Also, $\Delta\lambda$, the

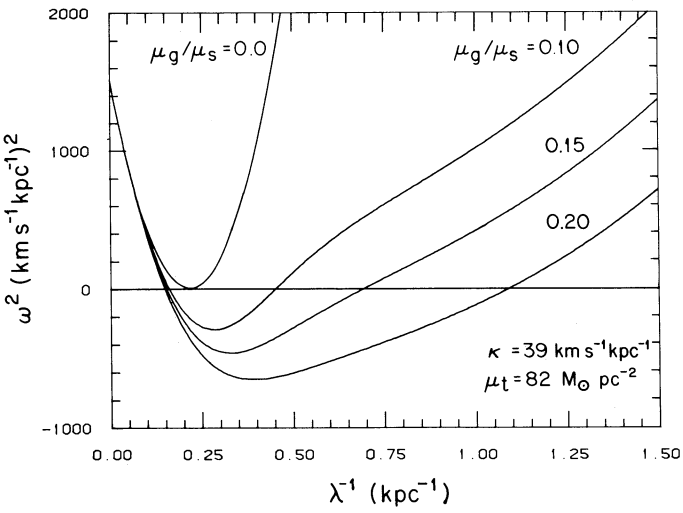

FIG. 3*a*

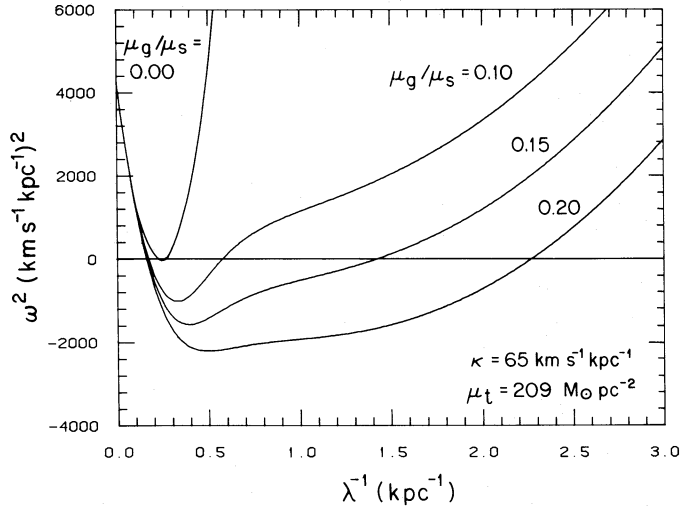

FIG. 3*b*

FIG. 3*a*.—Influence of the gas content on the instabilities in a two-fluid disk. ω^2 vs. λ^{-1} for the stars-alone system [$(\mu_g/\mu_s) = 0$] which has the same total density as the two-fluid curves, the latter drawn for $\mu_g/\mu_s = 0.10, 0.15$, and 0.20. $\kappa = 39$ km s^{-1} kpc^{-1} and $\mu_t = 82\ M_\odot$ pc^{-2}, giving $\mu_t/\kappa = 2.1\ M_\odot$ pc^2/km s^{-1} kpc^{-1}, $C_s = 25.2$ km s^{-1}. Even when only a small fraction of the density is put in a cold fluid, that is, gas ($\mu_g/\mu_s = 0.1$–0.2), an initially stable stars-alone system becomes unstable. As a result of increasing gas fraction (μ_g/μ_s); the most unstable mode grows faster, the most unstable wavenumber shifts to higher k values, and $\Delta\lambda$—the range over which two-fluid instabilities can occur—increases.

FIG. 3*b*.—Same as Fig. 3*a* but with higher $\mu_t/\kappa = 3.2\ M_\odot$ pc^{-2}/km s^{-1} kpc^{-1}, with $\kappa = 65$ km s^{-1} kpc^{-1} and $\mu_t = 209\ M_\odot$ pc^{-2}, $C_s = 39.0$ km s^{-1}. All the effects of the gas on the instabilities are stronger than in Fig. 3*a*. The dramatic increase in $\Delta\lambda$ for $\mu_g/\mu_s = 0.2$ in Fig. 3*b* is due to gas-alone approaching neutral equilibrium. Also, for this curve, the growth rate of the most unstable mode is nearly constant between $\lambda^{-1} = 0.3$ kpc^{-1} to 1.3 kpc^{-1}.

range of wavelengths over which two-fluid instabilities can occur, increases dramatically as μ_g/μ_s is increased from 0.1 to 0.2; this fact is probably very important in the evolution of the nonaxisymmetric perturbations. Note that the peak for ω^2 is nearly flat over a large range of wavelengths. This means that although technically one can still define a unique $k_{\rm peak}$; in reality, some other (nonlinear) mechanism may indicate another neighboring wavenumber as the most unstable mode. Indeed, the system may become unstable over a whole range of wavelengths simultaneously. Therefore, we expect gas-rich galaxies to show irregular features covering a large range of characteristic wavelengths, all due to gravitational instabilities.

Over moderate to high k values, most of the contribution to the formation of two-fluid instabilities comes from gas and this contribution is nearly independent of k (since $kC_g \ll \kappa$) as we will show in § III*c*. This causes the nearly flat nature of $\omega^2(k)$ over a large range covering intermediate to high k values for high μ_g/μ_s as seen here.

On comparing Figures 3*a* and 3*b*, we find that both the maximum growth rate of the two-fluid instability and $\Delta\lambda$ depend not only on μ_g/μ_s but also on μ_g/κ. In fact, the nearer the gas-alone system is toward becoming unstable by itself (as it is for $\mu_g/\mu_s = 0.15$ and 0.2 in Fig. 3*b*), the larger are $\omega^2_{\rm peak}$ and $\Delta\lambda$. We illustrate this in Figure 4, where the curves S and G represent the stars-alone and the gas-alone dispersion relations for the parameters corresponding to the curve S + G in Figure 3*b*. The curves S + G in Figure 4 are identical with the curves S + G in Figure 3*b*. For the sake of completeness we also include the case $\mu_g/\mu_s = 0.25$ (Fig. 4*d*).

Figures 4*c* and 4*d* respectively include the cases of gas-alone very slightly stable and gas-alone moderately unstable. In Figure 4*d*, $\Delta\lambda$, the range of unstable wavelengths for the two-fluid system, extends from $\lambda \sim 0.4$ kpc to about 5.0 kpc. The most unstable wavelength is near the most unstable gas-alone wavelength (at $\lambda \sim 0.7$ kpc), and the rate of growth is nearly constant between $\sim$0.5 kpc and 3.0 kpc. In Figure 4*c*, $\Delta\lambda$ extends from $\sim$0.45 kpc to 5.00 kpc. The maximum rate of growth is again constant over a large wavelength region (between 0.8 kpc and 3.0 kpc); however, the most unstable wavelength ($\lambda \sim 2.0$ kpc) lies near the most unstable stars-alone wavelength in this case. In Figure 4*b*, although the gas is having a strong influence on the two-fluid instabilities in terms of the peak growth rates and $\Delta\lambda$, the wavenumber for the two-fluid peak mode is well defined and is essentially stellar. This is because the joint contribution in this case peaks at low k as discussed in § III*c*.

The above results illustrating the importance of gas still hold good even if one were to draw Figure 3 for an initially quite stable stellar system. For example, if C_s used were 1.5 times the value necessary for neutral equilibrium for the stellar system [$(\mu_s)_{1\text{-}f} = (\mu_t)_{2\text{-}f}$], the two-fluid system would become unstable when μ_g/μ_s is only $\sim$0.25. In this case, $\Delta\lambda$ (for $\mu_g/\mu_s \sim 0.30$) extends from $\sim$0.6 to 3.0 kpc.

From Figures 1–4, we can see that a typical wavelength ($2\pi/k_{\rm peak}$) for a likely two-fluid instability is $\sim$2–3 kpc, and with μ_g as in Table 1, this yields the mass of gas in a typical two-fluid instability: $\sim 4 \times 10^7\ M_\odot$–$10^8\ M_\odot$.

From Figures 1–4, we can see that

$$(k_{\rm peak})_s < (k_{\rm peak})_{2\text{-}f} < (k_{\rm peak})_g\ ,$$

that is,

$$(\kappa/C_s) \lesssim (k_{\rm peak})_{2\text{-}f} \lesssim (\kappa/C_g)\ . \tag{29}$$

From these figures, especially Figure 4, we also see that for higher μ_g/μ_s values, $(k_{\rm peak})_{2\text{-}f}$ shifts more toward higher k values, thus approaching κ/C_g. The typical "low" and "high" values of k (given respectively by κ/C_s and κ/C_g) in the galaxy are $\sim$(2–3) kpc^{-1} and (8–16) kpc^{-1}, respectively, which correspond to wavelengths of 2–3 kpc and 400–800 pc.

As we will show in § III*c*, the shift to high k in $(k_{\rm peak})_{2\text{-}f}$ occurs at high μ_g/μ_s and specifically when the gas contribution dominates at all k so that the gas is primarily responsible for determining the most unstable wavenumber; hence in this case, $(k_{\rm peak})_{2\text{-}f}$ falls near κ/C_g. Note that such features would be evident in both the gas *and* the stellar system. This is a completely new range of wavenumbers for stellar system features that is opened up for investigation solely due to the two-fluid gravitational interaction inherent in the two-fluid analysis. Such small-scale features ($\lambda \sim$ 400–800 pc) are most likely to be seen in gas-rich galaxies and irregular galaxies. These features are also expected to occur at an early epoch in all galaxies, when galaxies are expected to be gas-rich. (See Paper II for a brief discussion of the connection between general two-fluid instabilities and galactic spiral structure.) Because of their large mass content, two-fluid instabilities will have a significant effect on heating up the stellar fluid in a galactic disk.

c) *Relative Contribution of the Two Fluids as a Function of μ_g/μ_s and k*

Recall from § II*d* that the two terms on the left-hand side of the criterion for the onset of two-fluid instabilities (eq. [27]) represent respectively the gaseous and stellar contributions to the formation of two-fluid instabilities. Hence, the relative contribution, γ, from the gas compared to that from the stars is given by:

$$\gamma = \frac{\mu_g(\kappa^2 + k^2C_s^2)}{\mu_s(\kappa^2 + k^2C_g^2)} \frac{|h_s[1 - \exp(-kh_g)]|}{|h_g[1 - \exp(-kh_s)]|}\ . \tag{30}$$

At any k, $\kappa^2 + k^2C_s^2 > \kappa^2 + k^2C_g^2$ for $C_s > C_g$. Also, since $h_s > h_g$, the ratio of the finite height reduction factors (given by the term in braces in eq. [30]) is greater than 1. Hence, γ is greater than μ_g/μ_s at any k. In other words, the contribution per unit surface density, μ, is larger for the gas than it is for the stars. Qualitatively, this point was noted earlier by Lynden-Bell (1967).

For the two-fluid case shown in Figure 1*a* [with $\mu_g/\mu_s = 0.1$ and $(k_{\rm peak})_{2\text{-}f} \approx 2.5$ kpc^{-1}], γ (from eq. [30]) is $\sim$0.33. Thus the contribution to the formation of instabilities is dominated by the stars in this case. Note, however, that the gas contribution is as high as 33% of the stellar contribution, even when the gas surface density is only about 10% of the stellar surface density.

This effect is attributed mainly to the lower gas velocity dispersion and to a much lesser degree to the lower scale-height of the gas as compared respectively to the velocity dispersion and the scale height of the stellar fluid. For low $k(\kappa/C_s < k \ll \kappa/C_g)$ the gas pressure term has a negligible effect on the total

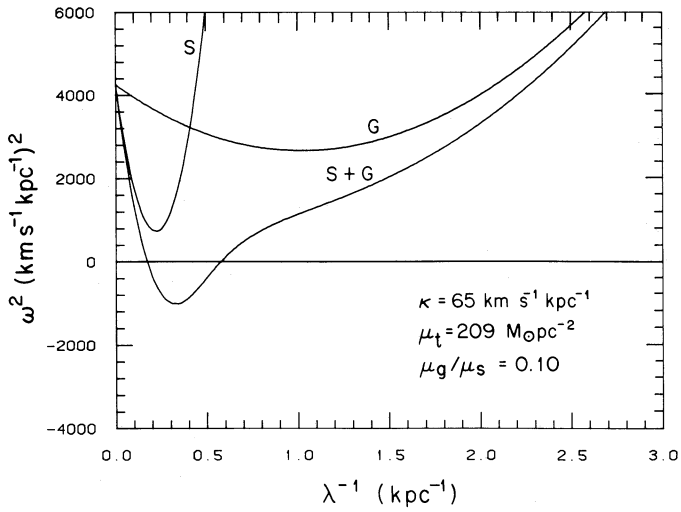

FIG. 4a

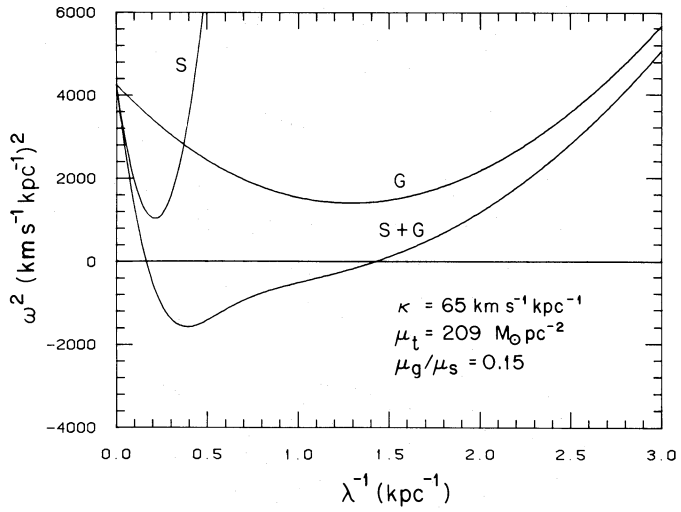

FIG. 4b

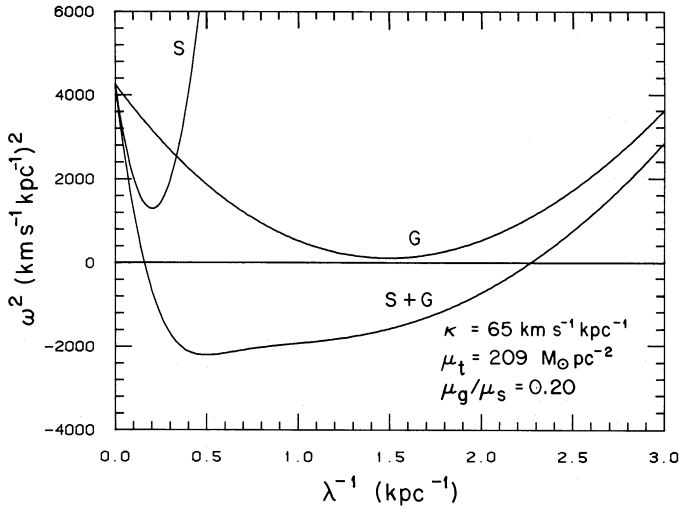

FIG. 4c

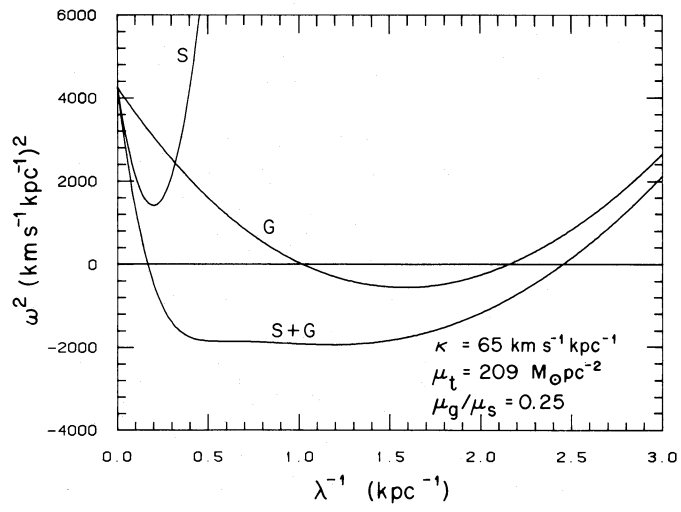

FIG. 4d

FIG. 4.—Comparison of separate one-fluid systems with the joint two-fluid system, as a function of the gas fraction (μ_g/μ_s) for μ_g/μ_s = (*a*) 0.10, (*b*) 0.15, (*c*) 0.20, and (*d*) 0.25. For Figs. 4*a*–4*d*, $\kappa = 65$ km s^{-1} kpc^{-1}, $\mu_t = 209\ M_\odot$ pc^{-2}, $C_s = 39.0$ km s^{-1}, and $C_g = 5$ km s^{-1}. The interaction of the two fluids is an increasing function of the gas fraction, μ_g/μ_s. Note that even though the stars-alone curve is very similar in Figs. 4*a* and 4*c*, the two-fluid curve has changed drastically—in the growth rate of the most unstable mode and in $\Delta\lambda$—as a result of $\sim 10\%$ shift of matter from stars to gas.

gas contribution since $k^2C_g^2 \ll \kappa^2$. Hence, for this range of k, equation (30) reduces to:

$$\gamma = \frac{\mu_g(\kappa^2 + k^2C_s^2)}{\mu_s\kappa^2}\left|\frac{h_s[1 - \exp(-kh_g)]}{h_g[1 - \exp(-kh_s)]}\right| . \qquad (31)$$

The lower scale height for the gas ($h_g < h_s$) further helps increase (though by less than $\sim 10\%$) the relative gas contribution at each k.

On increasing the gas fraction by a factor of 2.5 to 0.25, while keeping μ_t, C_s, and k constant, we find that the gas contribution is increased by a factor of 2.5 while the stellar contribution is lowered by a small factor ($\sim 15\%$), thus yielding equal contributions from each fluid ($\gamma \sim 1$). Thus, the gas contribution dominates ($\gamma > 1$), even at low k, for all $\mu_g/\mu_s > 0.25$, for the above input parameters. This results because the stars form a nondissipative (hence an incompressible) fluid while the gas is a compressible fluid. Hence $kC_g < \kappa$ at low k regardless of μ_g, and the relative contribution γ as given by equation (31) is correct even at moderately large μ_g/μ_s (<1) because of the effective near-independence of the velocity dispersion C_g on the surface density μ_g. The gas contribution dominates at the high k values since $C_s > C_g$ and since C_g is nearly independent of μ_g. At the high k value of $k = \kappa/C_g$, γ reduces to:

$$\gamma = \frac{\mu_g}{\mu_s}\frac{C_s^2}{2C_g^2}\left|\frac{h_s[1 - \exp(-kh_g)]}{h_g}\right| . \qquad (32)$$

The strong contribution from the gas to the two-fluid instabilities in the "stellar k regime" (small $k \sim \kappa/C_s$) that was seen above does not have its mirror equivalent in the stellar contribution in the "gaseous k regime" (large $k \sim \kappa/C_g$). Even neglecting the finite height correction (the braces in eq. [32]), equation (32) gives $\gamma > 1$ for $\mu_g/\mu_s > 2C_g^2/C_s^2$. For the set of parameters considered here, $C_g \sim 0.1$–$0.2C_s$, giving $\gamma > 1$ for $\mu_g/\mu_s > 0.08$–0.025. Only when μ_s/μ_g is extremely large ($> 1/0.08$–$1/0.025$ [$\gg 10$]) can γ be less than 1. Under these restrictions, the two-fluid system is effectively reduced to a one-fluid stars-alone system.

Thus, we can see that while the gas can affect the stability of the two-fluid system at low k significantly even when the gas fraction in the disk is only moderate ($\sim$0.1–0.2), the converse is not true; that is, the stars cannot affect the stability of the two-fluid system at large k, even at high μ_s/μ_g (~ 10). Even though we have treated both the fluids on an equal footing in the two-fluid analysis presented here, the two fluids do not exhibit symmetric behavior. Because of their high pressure and scale height, the stars have a negligible effect in the gaseous regime.

d) $\omega^2(k)$ with Four Real Roots

On closely examining the expression for $\omega^2(k)$ for the two-fluid case (eq. [20]), we find that it is a fourth order equation in k. Therefore, in the most general case, the above expression has four solutions for k. In each of the two-fluid curves plotted in Figures 1–4, only two solutions for k are real.

When all the four solutions for k are real, the plot of ω^2 versus λ^{-1} would appear as shown in Figure 5. Figure 5 depicts the behavior of a two-fluid system for the case where the two fluids interact feebly with each other and each fluid by itself is near its respective neutral equilibrium. The wavenumbers corresponding to the two fastest growing two-fluid perturbations fall close to $(k_0)_s$ and $(k_0)_g$, the neutral wavenumbers for stars and gas respectively. The stellar and gas contributions are seen to dominate strongly at low and high k values, respectively, and each fluid contributes little ($\lesssim$10–15%) at the k_0 corresponding to the other fluid. In fact, the values of the parameters used in plotting Figure 5 were "guessed," keeping the above criteria in mind.

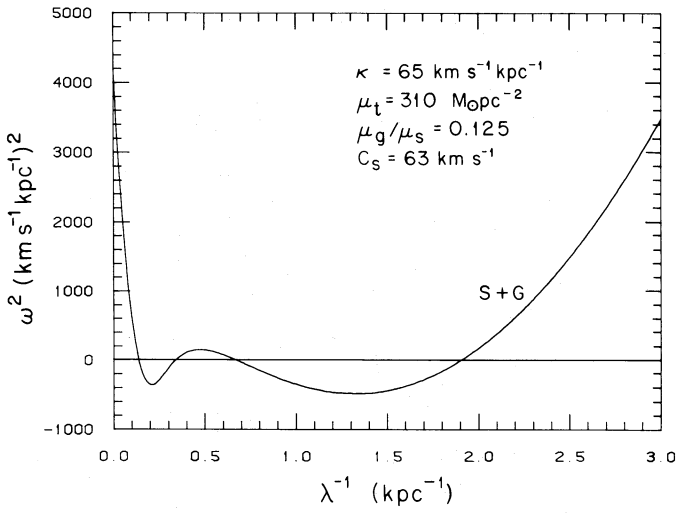

FIG. 5.—ω^2 versus λ^{-1} for the two-fluid case with four real roots. The parameters used for Fig. 5 are: $\kappa = 65$ km s^{-1} kpc^{-1}, $\mu_s = 275$ $M_\odot$ pc^{-2}, $\mu_g = 35$ $M_\odot$ pc^{-2}, $C_s = 63$ km s^{-1}, $C_g = 5$ km s^{-1}, $2h_s = 0.40$ kpc, $2h_g = 0.15$ kpc. The large values of μ_s, μ_t, and C_s restrict contribution from the stars at high k and the gas at low k to be $<15\%$ of the total contribution. The stellar and the gas contributions dominate at low k and high k values, respectively.

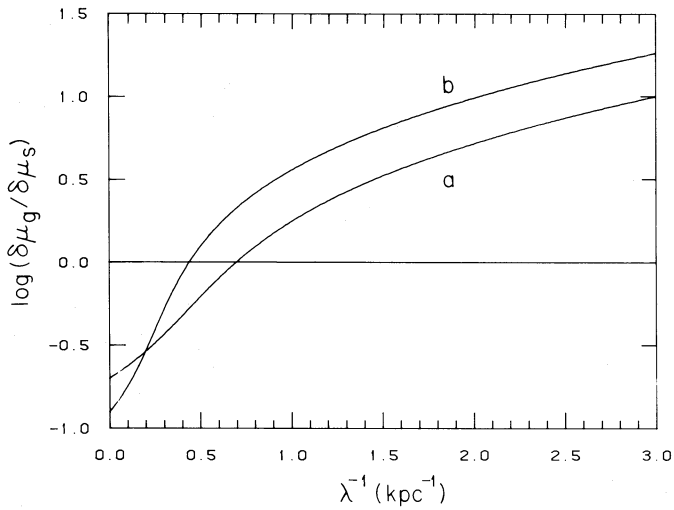

FIG. 6.—Logarithm of the amplitude in the gas to the amplitude in the stars versus k, for parameters corresponding to Fig. 4c (curve a) and Fig. 5 (curve b). In each case, the ratio of the amplitudes increases monotonically with k. The gas amplitude exceeds the stellar amplitude beyond $k \sim 4.4$ kpc^{-1} (curve a) and $k \sim 2.8$ kpc^{-1} (curve b).

In order to arrive at the plot drawn in Figure 5, we had to use rather unrealistically large values for μ_s, μ_t (and C_s), as can be seen by comparing the list of parameters for Figure 5 with Table 1 of Paper II. Were the observed values for these parameters to be used, one would get a plot of $\omega^2(k)$ versus k that has only two real k solutions (see the curve S + G in Fig. 1b). This constitutes an additional indirect evidence (corroborating earlier direct evidence, which consisted of $\gamma \sim 0.33$ for $(k_{\rm peak})_{2\text{-}f}$ in Fig. 1a) that leads us to the conclusion that the galaxy is a meaningful two-fluid system, so that the two fluids *do* interact substantially with each other and have comparable contributions to the formation of two-fluid instabilities.

e) Comparison of the Amplitudes in the Two Fluids

The amplitudes (that is, the perturbations in the surface densities) in the two fluids, for a given two-fluid perturbation mode, are not independent. This is because of the coupling of the two fluids that occurs via the force equation, as shown next. We can, therefore, obtain the ratio of the amplitude in the gas to that in the stellar fluid, $\delta\mu_g/\delta\mu_s$, for a given two-fluid mode (k, ω). Here $\delta\mu_g/\delta\mu_s$ is equal to $\delta\mu_g'/\delta\mu_s'$, the ratio of the (time-independent) magnitudes of the perturbed surface densities (see § IIb).

The linearized perturbation equations for the stars in a two-fluid system (eqs. [11], [13], [15], § II*b*) give:

$$\delta\mu_s' = \frac{\mu_{s0}[2\pi Gk(\delta\mu_s' + \delta\mu_g')]}{[\kappa^2 + k^2C_s^2 - \omega^2]} . \quad (33)$$

Similarly, the corresponding equations for the gas (eqs. [12], [14], [16], § II*b*) yield:

$$\delta\mu_g' = \frac{\mu_{g0}[2\pi Gk(\delta\mu_s' + \delta\mu_g')]}{[\kappa^2 + k^2C_g^2 - \omega^2]} . \quad (34)$$

Thus, the velocity dispersion of either fluid dictates its response to the joint gravitational perturbation. Combining equations (33) and (34), we obtain $\delta\mu_g/\delta\mu_s$ $(=\delta\mu_g'/\delta\mu_s')$:

$$\frac{\delta\mu_g}{\delta\mu_s} = \left(\frac{\mu_{g0}}{\mu_{s0}}\right)\left[\frac{\kappa^2 + k^2C_s^2 - \omega^2}{\kappa^2 + k^2C_g^2 - \omega^2}\right] . \quad (35)$$

Curves *a* and *b* in Figure 6 represent the plot of the logarithm of the above ratio versus k, for the parameters [including the output for $\omega^2(k)$] describing the two-fluid curves in Figure 4*c* (§ III*b*) and Figure 5 (§ III*d*), respectively. The above two cases represent the opposite extreme examples of strongly interacting two fluids (Fig. 4*c*) and weakly interacting two fluids (Fig. 5). From Figure 6, we see that, in each case $(\delta\mu_g/\delta\mu_s)$ is a monotonically increasing function of the wavenumber k. The gas amplitude is greater than the stellar amplitude at high k while the reverse is true at low k. The gas amplitude is dominant [i.e., $\log(\delta\mu_g/\delta\mu_s) > 0$] beyond $k \sim 4.4$ kpc^{-1} and 2.8 kpc^{-1} for the curves *a* and *b*, respectively.

Note that, for $|\omega^2| \ll \kappa^2 + k^2C_g^2$, the ratio of the amplitudes (eq. [35]) is identical to γ, the ratio of the contributions from the two fluids (eq. [30], § III*c*), neglecting the finite height correction (that is, the term in braces in eq. [30]). Now, for cases *a* and *b*, the wavenumbers at which the amplitude in the gas equals the amplitude in the stars, do have low associated $|\omega^2|$ $(<\kappa^2)$, as seen from Figures 4*c* and 5, respectively. Therefore, γ is expected to be ~ 1 at these wavenumbers. In fact, we do obtain $\gamma \sim 1.30$ (at $k \sim 4.4$ kpc^{-1}, case *a*) and $\gamma \sim 1.00$ (at $k \sim 2.8$ kpc^{-1}, case *b*), thus proving that the amplitude in the gas exceeds the amplitude in the stars when the gas contribution exceeds the stellar contribution and vice versa. This is seen clearly in Figure 5, where the wavenumber beyond which the amplitude in the gas dominates ($k \sim 2.8$ kpc^{-1}, case *b*, Fig. 6) lies in the intermediate k-range (of stable modes) which separates the low and high k regions to which the contributions from the stars and the gas respectively are nearly exclusively limited.

Equation (35) is valid only as long as $(\delta\mu_s/\delta\mu_{s0}) \leq 1$, as explained in § III*a*, Paper II. Equation (35) is important for comparison with the observations of the amplitudes, of features of same wavelength in the two fluids. However, due to the nonlinear evolution of gas, the actual comparison with observations is tricky and we do not attempt it here.

IV. CONCLUSIONS

We have formulated a two-fluid scheme wherein the stars and the gas in a galactic disk are represented as two isothermal fluids and the *two fluids interact gravitationally with each other*. The disk is supported by rotation and random motion. We have studied the characteristics of two-fluid gravitational instabilities.

The main conclusions from this paper are:

1. Even when both the fluids (that is, the gas and the stellar fluid) in a two-fluid system are stable when considered separately, the resulting joint two-fluid system may be neutrally stable (Fig. 2) or even *unstable* to the growth of the two-fluid gravitational instabilities (Fig. 4*a*). This is due to the additional gravitational self-energy in the (two-fluid) system resulting from the gravitational interaction between the two fluids. The gas in a galactic disk, even when it is only a fraction of the total surface density, affects the stability of the entire disk including the stars.

2. For any galactic disk, the contribution per unit surface density, μ, toward the formation of two-fluid instabilities is larger for the gas than it is for the stars. This is due to the lower velocity dispersion of the gas compared to that of the stars. Therefore, the galaxy at the current epoch is a meaningful two-fluid system in that the contributions from the two fluids are comparable for the observed gas fraction $(\mu_g/\mu_s = 0.1\text{–}0.2)$. At high wavenumbers, the gas contribution always dominates.

3. The ratio of the amplitude in the gas to the amplitude in the stars is a monotonically increasing function of the wavenumber of the two-fluid perturbation. For marginally unstable or stable two-fluid modes $(|\omega^2| \ll \kappa^2 + k^2C_g^2)$, the gas amplitude exceeds the stellar amplitude when the gas contribution exceeds the stellar contribution and vice versa.

4. The wavelength of a typical two-fluid instability in the inner galaxy [for gas fraction $(\mu_g/\mu_s) = 0.1\text{–}0.2$] is $\sim$2–3 kpc. The mass of gas in a typical two-fluid instability in the disk is $\sim 4 \times 10^7\text{–}10^8\ M_\odot$. The addition of gas in our two-fluid analysis reduces the wavelength even for the stellar system from its one-fluid Toomre value.

In general the most unstable two-fluid wavenumber increases with increasing gas fraction and lies between the limits $\kappa/C_s < (k_{\rm peak})_{2\text{-}f} < \kappa/C_g$. Both the stars and the gas will have features with characteristic wavelengths $2\pi/(k_{\rm peak})_{2\text{-}f}$. For the Galaxy this corresponds to between $\sim$2.5 and $\sim$0.5 kpc. This "new" range of wavelengths near that of the gas-alone case ($\lambda \sim 0.5$ kpc) is expected in gas-rich galaxies and also in all galactic disks in an early stage of their evolution.

The typical growth rate for a two-fluid instability in the Galaxy is a few times 10^7 years. The rate of growth of the most unstable two-fluid perturbation mode is an increasing function of μ_g/μ_s and μ_t, the total disk surface density.

Because of their large mass content, two-fluid instabilities will have a significant effect on heating up the stellar fluid in a galactic disk.

APPENDIX A

SELF-GRAVITATIONAL FORCE IN THE GAS

Toomre (1964) and Goldreich and Lynden-Bell (1965) find that a given fluid that is uniformly distributed in a flattened but finite height disk and that is supported by the random motion of the particles in the fluid and by the

TABLE 2

SELF-GRAVITATIONAL FORCE IN THE GAS

R (kpc)	κ[a] (km s^{-1} kpc^{-1})	$\mu_g(H_2)$ ($M_\odot$ pc^{-2})	$\mu_g(H_2) + \mu_g(H\ I)$ ($M_\odot$ pc^{-2})	$(\mu_g)_{total}$[b] ($M_\odot$ pc^{-2})	Q_g[c] at $C_g = 5$ km s^{-1}	Q_g[c] at $C_g = 8$ km s^{-1}
4	89	6.6	9.6	13.4	2.21	3.54
5	74	11.8	14.8	20.7	1.20	1.92
6	65	17.3	20.3	28.4	0.77	1.23
7	57	12.2	15.2	21.2	0.90	1.43
8	49	8.5	11.5	16.1	1.03	1.64
9	44	5.1	8.1	11.3	1.29	2.06
10	39	3.6	6.6	9.2	1.41	2.26

[a] The values for κ, the epicyclic frequency, are from Caldwell and Ostriker 1981.
[b] $(\mu_g)_{total} = 1.4[\mu_g(H_2) + \mu_g(H\ I)]$, for 10% He number fraction.
[c] Q_g = Toomre Q-factor for the stability of a gas disk
$= \kappa C_g/[3.36G(\mu_g)_{total}]$.

differential rotation in the galaxy is gravitationally unstable to the growth of cylindrically symmetric perturbations in it if

$$(\mu_g)_{total} \geq \left(\frac{\delta\kappa C_g}{3.36G}\right) \tag{A1}$$

where $(\mu_g)_{total}$ is the total observed surface mass density of the gas in the galaxy. The parameter δ depends on the equation of state of the fluid and on the ratio of the vertical scale height to the planar length-scale of the gravitational instability; the value of δ is $\sim 1(\pm 50\%)$ for the different cases. For the semiquantitative analysis proposed here, we set $\delta = 1$. Equation (A1) then reduces to

$$Q_g = \frac{\kappa C_g}{[3.36G(\mu_g)_{total}]} \leq 1\ , \tag{A2}$$

where Q_g is the Toomre Q-factor for the stability of one-fluid gas disk.

The total gas surface density $(\mu_g)_{total}$, including H_2, H I, and He components (with He being 10% by number fraction), is given by $1.4[\mu_g(H_2) + \mu_g(H\ I)]$. The observational values for $\mu_g(H_2)$ are taken from Sanders, Solomon, and Scoville (1984) and Sanders (1982). For H I, we adopt a constant midplane density of 3 $M_\odot$ pc^{-2} (Burton 1976). In § III*a*, we describe the observed range of values for C_g in the disk. The last two columns in Table 2 list the values for Q_g (eq. [A2]), given as a function of R, for $C_g = 5$ km s^{-1} and 8 km s^{-1}, respectively.

These results for Q_g show that, by itself, the gas in the Galaxy is not unstable to the growth of gravitational perturbations in it, except perhaps for lower C_g values ($\lesssim 5$ km s^{-1}) for the intermediate region (R = 5–8 kpc) in the Galaxy. Even this range, where the gas is more prone to becoming unstable, is further reduced (to R = 6–7 kpc) when the reduction (up to $\sim 30\%$) in the effective gas density due to the finite gas scale height is taken into account, and this range could vanish completely since the observational data for $\mu_g(H_2)$ is uncertain by as much as a factor of 2. Hence the above results suggesting the possible existence of gas instabilities for the intermediate R-values in the Galaxy are too close to the satisfaction of the instability criterion for them to be definitely reliable.

APPENDIX B

FINITE AND DIFFERENT SCALE HEIGHTS OF THE TWO FLUIDS

i) A thin disk of finite height cannot be converted to a closed geometrical distribution of matter (such as, for example, a sphere or a series of concentric ellipsoids) by any series of geometric transformations. Hence the contribution of a disk of finite height to $\partial_r \delta\phi$ along the $z = 0$ plane can be nonzero. Applying the same argument separately to each of the two fluids in a system of two fluids (with $2h_s > 2h_g$), it is clear that even when the two fluids have different scale heights, the radial force component at $z = 0$ due to the stellar fluid can be nonzero and hence it *can* affect the gaseous fluid via the force equation and vice versa. This point is crucial in order that the fluids do interact gravitationally in the plane of the disk even though they have different scale heights.

ii) Although two-fluid instabilities can exist even when the two fluids have different z scale heights, the instability analysis in § II is strictly valid only for a subset of the possible modes, because of the following technical point.

The form of the Poisson equation (eq. [9]) and the resulting radial perturbation force at $z = 0$ (eq. [10]) are strictly valid for a thin disk, that is, when $2h \ll \lambda$, where λ = the length scale of the instability.

This choice clearly fails in the extreme opposite limit when $\lambda \ll 2h$. In this case physically it is clear that one is moving into the Jeans regime, that is, to a three-dimensional homogeneous matter distribution, at least on a length scale of $\sim\lambda$. That

this is true mathematically also, can be checked easily. The dispersion relation for a one-fluid system ($h \neq 0$) is given by equation (25); see § II*d*. For $(2h/\lambda) \to \infty$, this reduces to:

$$\omega^2 = \kappa^2 + k^2C^2 - (2\pi Gk\mu/kh) = \kappa^2 + k^2C^2 - 4\pi G\rho \,, \tag{B1}$$

which is the familiar Jeans relation, when κ^2 is negligible. Here $\rho = \mu/2h$ is the volume density and $2h$ is the total scale height of the disk.

For an intermediate finite value of (h/λ), the above choice is correct; however, the effective $\delta\phi$ is lower due to the nonrigorous choice of the Poisson equation and its solution. (Note that this decrease in the gravitational potential is over and above the reduction implied by the effective reduction in the surface density due to the finite height).

For most of the two-fluid cases considered in this study, the fastest growing modes have wavelengths much larger than $2h_s$ $(> 2h_g)$; hence the two-fluid analysis described here is accurate for these modes in which we are primarily interested.

REFERENCES

Berman, R. H., and Mark, J. W.-K. 1977, *Ap. J.*, **216**, 257.
Burton, W. B. 1976, *Ann. Rev. Astr. Ap.*, **14**, 275.
Caldwell, J. A. R., and Ostriker, J. P. 1981, *Ap. J.*, **251**, 61.
Cowie, L. L. 1980, *Ap. J.*, **236**, 868.
Elmegreen, B. G. 1979, *Ap. J.*, **231**, 372.
———. 1982*a*, *Ap. J.*, **253**, 634.
———. 1982*b*, *Ap. J.*, **253**, 652.
Goldreich, P., and Lynden-Bell, D. 1965, *M.N.R.A.S.*, **130**, 97.
Gordon, M. A., and Burton, W. B. 1976, *Ap. J.*, **208**, 346.
Hunter, C. 1972, *Ann. Rev. Fluid Mech.*, **4**, 219.
Innanen, K. A. 1973, *Ap. Space Sci.*, **22**, 393.
Jog, C. J., and Solomon, P. M. 1984, *Ap. J.*, **276**, 127 (Paper II).
Kwan, J. 1979, *Ap. J.*, **229**, 567.
Listz, H. S., and Burton, W. B. 1981, *Ap. J.*, **243**, 778.
Lynden-Bell, D. 1967, in *Lectures in Applied Mathematics*, Vol. **9**, ed. J. Ehlers (Providence: American Mathematical Society), p. 131.
Mihalas, D., and Binney, J. 1981, *Galactic Astronomy* (San Francisco: Freeman), p. 422.
Sanders, D. B. 1982, Vancouver Workshop on Galactic Structure and Dynamics.
Sanders, D. B., and Solomon, P. M. 1984, in preparation.
Sanders, D. B., Solomon, P. M., and Scoville, N. Z. 1984, *Ap. J.*, **276**, in press.
Scoville, N. Z., and Hersch, K. 1979, *Ap. J.*, **229**, 578.
Scoville, N. Z., and Solomon, P. M. 1975, *Ap. J.* (*Letters*), **199**, L105.
Solomon, P. M. 1981, in *NRAO Workshop on Extragalactic Molecules*, Green Bank, W. V., ed. M. Kutner and L. Blitz, p. 61.
Solomon, P. M., Barett, J., Sanders, D. B., and de Zafra, R. 1983, *Ap. J.* (*Letters*), **266**, L103.
Solomon, P. M., and Sanders, D. B. 1980, in *Third Gregynog Astrophysics Workshop, Giant Molecular Clouds in the Galaxy*, ed. P. M. Solomon and M. G. Edmunds (Oxford: Pergamon Press), p. 41.
Solomon, P. M., Sanders, D. B., and Scoville, N. Z. 1979, in *IAU Symposium 84, The Large Sclae Characteristics of the Galaxy*, ed. W. B. Burton (Dordrecht: Reidel), p. 35.
Solomon, P. M., Scoville, N. Z., and Sanders, D. B. 1979, *Ap. J.* (*Letters*), **232**, L89.
Spitzer, L. 1978, *Physical Processes in the Interstellar Medium* (New York: Wiley), p. 231.
Stark, A. A. 1979, Ph.D. thesis, Princeton University.
Talbot, R. J., and Arnett, W. D. 1975, *Ap. J.*, **197**, 551.
Toomre, A. 1964, *Ap. J.*, **139**, 1217.
Young, J. S., and Scoville, N. Z. 1981, *Ap. J.*, **258**, 467.
———. 1982, *Ap. J.*, **258**, 457.

CHANDA J. JOG: Princeton University Observatory, Peyton Hall, Princeton, NJ 08544

P. M. SOLOMON: Astronomy Program, State University of New York at Stony Brook, Stony Brook, NY 11794